Biomicrofluidics PERSPECTIVE pubs.aip.org/aip/bmf

Opportunities of scalable and electrostatically optimized electrodes for electric field- and current-driven microfluidic applications

Cite as: Biomicrofluidics 19, 031302 (2025); doi: 10.1063/5.0244129
Submitted: 16 October 2024 · Accepted: 25 March 2025 ·
Published Online: 2 May 2025

View Online Export Citation CrossMark

K.-S. Csizi,[1] A. E. Frackowiak,[1,2] R. D. Lovchik,[1] and E. Lörtscher[1,a)]

AFFILIATIONS

[1]IBM Research Europe—Zurich, Säumerstrasse 3, CH-8804 Rüschlikon, Switzerland
[2]Department of Chemistry, University of Basel, St. Johans-Ring 19, CH-4056 Basel, Switzerland

[a)]**Author to whom correspondence should be addressed:** eml@zurich.ibm.com

ABSTRACT

Silicon-based microfluidics enable the creation of highly complex, three-dimensional fluid networks. These comprise scalable channel sizes and monolithically integrated functionalities available from complementary–metal–oxide–semiconductor technology. On this versatile, solid-state platform, advanced manufacturing techniques exist that allow the channel walls to be directly electrified with one or multiple pairs of electrodes along the fluid-carrying channel. The electrodes have ideal electrostatic geometries, yielding homogeneous electric field distributions across the entire cross section of the microfluidic channel. As these are located directly at the channel, only low supply voltages are needed to achieve suitable field strengths. Furthermore, a controlled supply of charge carriers to the microfluidic channel is feasible. These configurations may serve numerous applications, including highly efficient mechanisms to manipulate droplets, cells, and molecular compounds, perform pico-injection or poration, trigger and control chemical reactions, or realize electrochemical and capacitive sensing modalities. In this perspective, we describe the generic design and fabrication of these electrodes and discuss their miniaturization and scaling properties. Furthermore, we forecast novel use cases and discuss challenges in the context of the most interesting applications.

© 2025 Author(s). All article content, except where otherwise noted, is licensed under a Creative Commons Attribution-NonCommercial-NoDerivs 4.0 International (CC BY-NC-ND) license (https://creativecommons.org/licenses/by-nc-nd/4.0/). https://doi.org/10.1063/5.0244129

I. INTRODUCTION

Silicon has been the key enabling material for the development of integrated circuits and other Complementary–Metal–Oxide–Semiconductor (CMOS) components up to now. Over the last few decades, the continuous development and process improvements simultaneously enabled steady miniaturization and an increase of functionalities from analog building blocks and circuits in the early days of computing to native artificial intelligence hardware these days. Silicon, however, is also a very favorable material to directly create microfluidic devices as it is mechanically compliant, chemically resistant against most chemicals, has no fatigue, and can be cleaned under harsh conditions to permit the reuse of the devices. Furthermore, feature sizes are scalable from hundreds of micrometers down to just a few tens of nanometers on the same wafer using lithographic techniques. Various surface functionalization and passivation techniques exist in advanced semiconductor manufacturing that can directly be deployed, e.g., to tune surface wettability or the chemical surface resistance. In addition to the fabricational overhead, it does, however, neither allow diffusion of oxygen, as is the case with polydimethylsiloxane (PDMS), for instance, nor is it flexible at normal wafer thicknesses or transparent at visible or near-infrared wavelengths. Instead, silicon chips can be stacked by anodic or fusion bonding, to form complex three-dimensional fluid networks, while various CMOS functionalities can be monolithically integrated. Also, hybrid PDMS–silicon chips have been realized that combine the advantages of both materials.

II. ELECTRODES AS ACTUATORS, TRIGGERS, AND SENSORS IN MICROFLUIDICS

Microfluidic devices provide means to precisely handle minuscule amounts of fluids by operating in channels or similar flow-confining structures with dimensions somewhere between some hundreds down to a few micrometers or even nanometers. Within these channels, the flow dynamic properties can be tailored to

© Author(s) 2025

manipulate liquids, gases, or other objects contained therein and/or to trigger various processes. This includes, e.g., the creation and manipulation of emulsion droplets, a subfield referred to as droplet microfluidics. In this approach, the droplets define a reaction compartment themselves, comprising cells, vesicles, exosomes, deoxyribonucleic acid (DNA)/ribonucleic acid (RNA), proteins, or small single molecules. Among a variety of mechanisms, electric fields play an important role because they can induce electrophoretic effects that lead to polarization and, thus, allow field-induced manipulation of polarized objects, including droplets. The most prominent applications, among many, are injection of one droplet into another droplet as well as droplet deflection, the latter of which also allows droplet sorting. All of these electrophoretic effects depend directly on the field amplitudes that can be generated across the channel's cross section. The time ramp to achieve a given field strength (E) directly determines the speed of operation as the voltage patterns mostly oscillate at fixed frequencies or controlled by a triggering event. For example, high-throughput sorting based on fluorescence-based closed-loop feedback can be achieved at 1 kHz droplet sorting frequency or more. Based on the aforementioned considerations, it becomes obvious that the lower the supply voltage, V_{Supp}, to achieve a given field strength, the faster the system can be operated since the temporal voltage rise or descent is physically limited in voltage sources.

Apart from functioning as actuators for manipulation, electric fields can also be used for injection or poration, both applications depending again on the amplitude achievable at the desired location within the channel. To achieve electric fields, various methods are feasible; in addition to the physical implementation of electrodes in the microfluidic device body, also, optical fields can be used for all the functions described above, acting as optoelectronic tweezers. Similarly, surface acoustic waves[1] can also be used for manipulation while being implemented in the microfluidic device. While this perspective focuses on the physical implementation of electrodes and their scaling properties, the opportunities of optoelectronic tweezers are described elsewhere.[2] Compared to these electro-optical triggers, physical electrodes are also attractive components beyond inducing electric fields because they can supply electrons (and holes) to the channel, thereby acting as electrochemical reaction triggers. Conversely, electrodes allow for electrical measurements between a ground element and one or multiple counterelectrodes. This provides the means to directly or indirectly sense objects passing the electrodes in the channels. Here, the closer the electrodes are to the analytes, the higher the sensitivity and/or the temporal and spatiotemporal resolution.

III. DIRECT ELECTRIFICATION OF CHANNEL WALLS

Achieving suitably high field strengths and/or sensitive electrical measurements across the channel is key to the above operations. In turn, optimal electrostatic conditions reduce the supply voltage for highly efficient operation, thereby enabling the highest switching frequencies and high throughput. From an electrostatic and fluid-dynamic point of view, the optimal position of electrodes is directly in the microfluidic channel walls. However, the placement of electrodes along microfluidic channels has been a major challenge in the field as there always seemed to be a compromise between field homogeneity across the channel and the remote alignment of the electrodes, which defines the field strengths and operating voltages. For example, thin-film electrodes have been patterned on a glass[3] or a silicon chip that was subsequently bonded to a PDMS chip containing the channels. This allowed for closely spaced electrodes but resulted in highly inhomogeneous field distributions, large gradients, and channel-internal field hot-spots. More symmetrical geometries were created by placing electrodes in auxiliary channels in the PDMS corpus, filled with conductive materials, such as low-melting point solders,[4,5] silver paste,[6] or ionic liquids, including salt water.[7] Other geometries resulted in electrodes at a height similar to the channel.[8,9] For all these approaches, the electrodes cannot be placed arbitrarily close to the microfluidic channel due to fabrication tolerances, sealing and insulation requirements, a hurdle that has been overcome in metal–PDMS composites.[10–12] The conductivity of these elements, however, is difficult to control. Recently, we developed an approach to directly electrify the channel walls of silicon microfluidic devices.[13,14] It overcomes all of the above drawbacks and bears great potential for scaling and applications, including pico-injection, droplet deflection, or sorting. Here, we describe the fabrication, scaling, and operation principles.

A. Fabrication

The approach to electrify the walls of a silicon microfluidic channel to form electrodes is based on local oxidation of the top (device) layer of silicon-on-insulator (SOI) wafers [Fig. 1(a)], composed of silicon, into silicon dioxide (SiO_2). The initial height of the silicon layer ("device layer") later defines the microfluidic channel height [Fig. 1(b)], and its conductivity can be chosen to vary from pristine/undoped to highly doped silicon depending on the application, as will be discussed later. To define the segments where the device layer should become electrically insulating to separate the electrified areas from the bulk or neighboring ones, vertical access through the entire device layer must be established for the ions to oxidize the surrounding silicon surfaces. This is realized by deep reactive ion etching (DRIE) of a perforation pattern (e.g., holes or rectangles, perforation size d with a pitch p in separation) using a resist or a hard mask to protect the remaining area [Figs. 2(a) and 2(b)]. Thermal oxidation is a self-limiting process as the silicon converted to silicon oxide becomes less and less permeable to oxygen at thicknesses beyond $\approx 1\,\mu$m. The process is rather slow [(30–80) nm/h] and hence highly controllable. As a result of the oxidation, all the segments between the perforation openings become oxidized [Fig. 2(c)] and thus electrically insulating. Figure 2(d) shows the top view of the resulting electrode patterning process with the design parameter for the insulating width, $w = d + 2 \times l$ where d is the transversal dimension of the perforation and l is the extent of the surrounding oxidation layer, respectively. As a last step, the top oxide is removed to guarantee proper anodic bonding to a glass cover. Alternatively, the DRIE step used to define the microfluidic channels (and openings for oxidation) can also be used to directly open trenches between the electrode segments, which can then be filled conventionally with so-called "high-k" dielectric materials [dielectric constant higher than 3.9 (thermally grown SiO_2)], such as Si_3N_4, Al_2O_3, HfO_2, TiO_2, etc.,

© Author(s) 2025

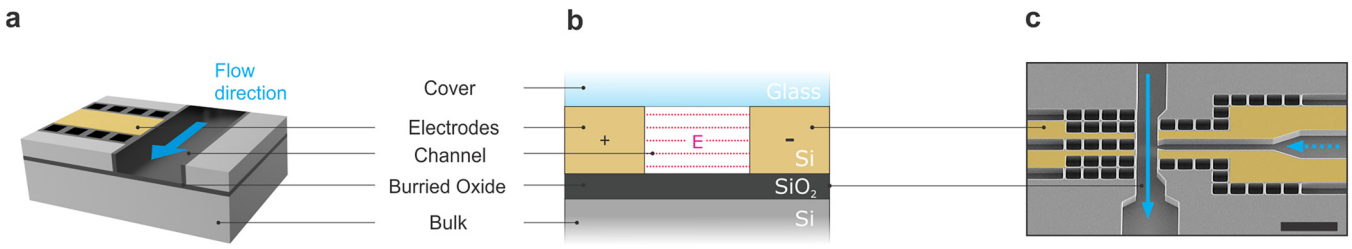


FIG. 1. Schematic representation of the direct electrification of silicon microfluidics: (a) Oxidized perforation patterns enable sections of the silicon layer to become electrically insulated from the rest of the channel walls, including the bottom and top ones, resulting in an electrically addressable wall segment transversal to the flow direction (light blue arrow). (b) Cross-sectional view through one channel depicting the homogeneous electric fields with two opposite electrodes. (c) Scanning-electron microscopy image of a device with two electrode pairs. An additional channel protrudes from the right (dotted light blue arrow) as this specific device is used for pico-injection. Scale bar: 100 μm. Adapted from Fig. 2 of Monserrat Lopez *et al.*, Microsyst. Nanoeng. **9**, 81 (2023); licensed under a Creative Commons Attribution (CC BY) license. Copyright 2023 Author(s), licensed under a Creative Commons Attribution (CC BY) License.

by using, for instance, atomic layer deposition, chemical vapor deposition, etc. Compared to SiO_2, such high-k dielectrics would provide means to increase the break-down voltage for high-tension operation or to lower the electrode spacing. Therefore, the electrodes can be positioned even closer, which is highly beneficial for some of the applications envisioned in Sec. IV. Irrespective of the deposition or growth technique used, the wafer structure must last be planarized, e.g., by chemical–mechanical polishing or ion-milling, to again enable proper anodic bonding of the cover glass. Optionally, the handle wafer can be partially removed underneath the channels by etching from the backside, a process that requires only one additional lithographic step followed by DRIE. This then provides an optical view port for transmission experiments, e.g., needed for fluorescence-based droplet sorting or other widely used spectroscopic techniques. Depending on the application, the thickness of the buried oxide in the SOI stack can be chosen between a few tens of nanometers and some micrometers. Hence, an optimal trade-off between mechanical stability and optical performance can be found. Still, the lateral dimensions of the windows should be kept minimal to avoid cracking thereof, especially when operating at higher pressures or low-viscosity media. For conventional microscopy, the field of view enabled by these viewports, however, is sufficiently large, also to achieve proper conditions for illumination and light harvesting.[14] All the details of the fabrication

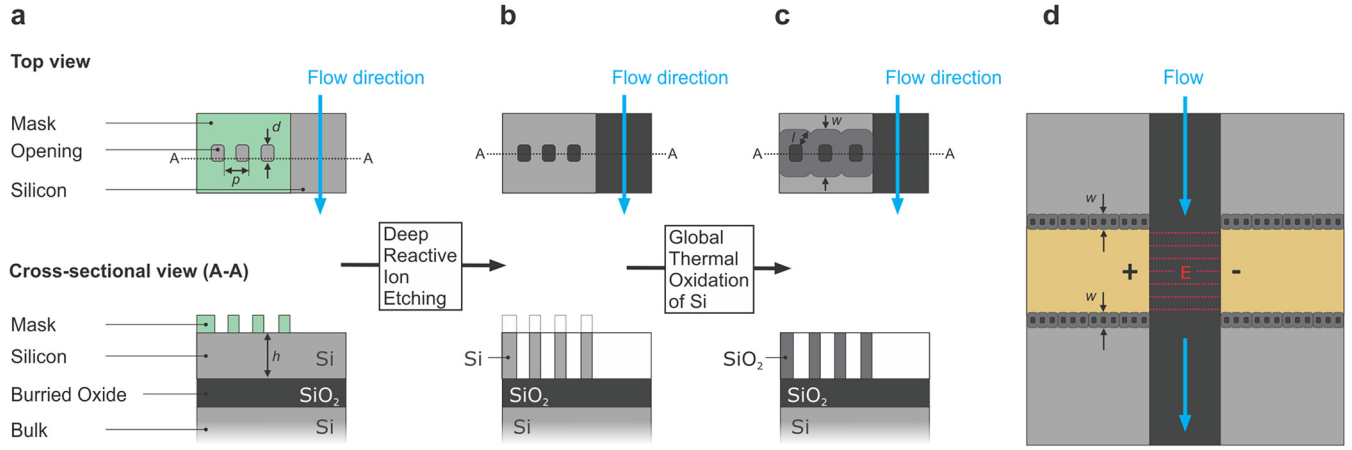


FIG. 2. Rational design and fabrication steps for realizing wall-embedded electrodes in silicon microfluidics: Top view (upper row) and cross-sectional view (bottom row) of the three main fabrication steps. (a) Starting with masking (green) the silicon-on-insulator (SOI) stack to expose the channel and perforation segments of diameter d and pitch p to reactive ion etching across the entire silicon layer of height h while protecting the masked area. (b) Channels and perforations are etched simultaneously in this self-aligned process that is automatically stopped at the buried oxide layer. (c) The self-limited thermal oxidation of silicon penetrates for a certain length l into the silicon bulk, therefore, creates insulating segments, located in between the perforations elements (c). The sum of the initial perforation size, d, and twice the oxidation length, l, defines the width of the insulating segment, $w = d + 2 \times l$. (d) Generic layout depicting the total area occupied for one electrode pair as defined by the insulation widths and the area in between them. Adapted from Fig. 2 of Monserrat Lopez *et al.*, Microsyst. Nanoeng. **9**, 81 (2023); licensed under a Creative Commons Attribution (CC BY) license. Copyright 2023 Author(s), licensed under a Creative Commons Attribution (CC BY) License.

© Author(s) 2025

process, including electrical characterization of the insulating barriers, can be found in the corresponding publication.[14]

B. Scaling properties

Both from a fabrication and performance point of view, the electrification concept bears great potential for different scaling. For the initial proof-of-concept, typical microfluidic dimensions were chosen, specifically $h = 27.5\,\mu m$, $w = (20–100)\,\mu m$, $d = (10–15)\,\mu m$, and $p = 2\,\mu m$. An etching time corresponding to an oxidation width $l = 1.5\,\mu m$ fully isolated the segments, yielding an electrical resistance of 0.1–1 TΩ.[14] With these dimensions, the supply voltage for pico-injection, droplet deflection, and sorting could be reduced by 2–3 orders of magnitude compared to state-of-the-art approaches. Despite this low-voltage operation, operating at sorting frequencies of 0.7 kHz was achieved, which is between the high-throughput (0.5 kHz) and ultrahigh-throughput (2 kHz) regimes (most likely limited by the speed of the optical signal processing logic of the field-programmable gate-array[14] rather than the electrode driving conditions.) Given the rather moderate spatial dimensions for nanofabrication, it shall be discussed in this perspective how the electrification concept can be further scaled in different directions:

i. *Downscaling and miniaturization of dimensions*: Reducing the device layer height or channel height and/or the width of the channels.
ii. *Increasing the electric field strengths*: As silicon does not diffuse under high-field conditions, much larger supply voltages than previously used are feasible, resulting in electric field strengths of 10^6–10^8 V/m.
iii. *Increasing the number of electrodes*: Multiple electrodes can be placed along the channel, separated only by the insulating barrier of width w.
iv. *Increasing the electric-field gradients*: In addition to the homogeneous electric field distributions, created, for instance, between two opposite electrodes as depicted in Fig. 1(b), more complex field distributions can also be realized. By stacking two layers on top of each other (Fig. 3 central illustration), a quadrupolar field arrangement can be established. Non-symmetric electrode arrangements across the channels lead to field gradients highly suitable for deflection [see Fig. 1(c)].

For the miniaturization of all relevant dimensions as well as for the spatial separation of the electrodes along the channel, the scaling properties of the insulating barriers and the underlying fabrication mechanisms must be taken into account. For the patterning of the masks that allow the perforations to be created, the transition from ultraviolet (UV) photolithography to electron-beam or even ion-beam lithography will allow for sub-100 nm feature sizes. Direct opening of a hard mask by focused ion-milling will even allow sub-10 nm holes to be created, at least for thin mask layers. For etching perforations into the silicon device layer, the aspect ratio of channel height and perforation size, $r = h/d$, must be further considered; regardless of the approach, highest values range somewhere between 50 and 100. Hence, nanometric insulating barriers can be envisioned for micrometer-sized channel dimensions using the thermal oxidation approach described above. Alternatively, high-k dielectrics as insulating materials may lead to even smaller separation between the electrode segments along the channels, enabling various novel applications as described in Sec. IV. Furthermore, nanochannels are also interesting for functionalization with arrays of nanoelectrodes, as they offer attractive opportunities for sensing, despite the generally limited flow rates in nanochannels. Here, even smaller perforations and widths are possible as the device layer is correspondingly thinner. For all of the above highly generic device concepts and the scaling properties thereof, it shall be noted that silicon does not become diffusive even under high-field conditions and that the electrical break-down voltage around 10 MV/cm for thermally grown silicon oxide is among the highest values reported for oxides. Furthermore, as long as only electric fields are desired, pristine silicon is perfectly suited and can be used directly. However, if charge carriers shall be supplied to the channels, e.g., as reagents for electrochemical reactions,

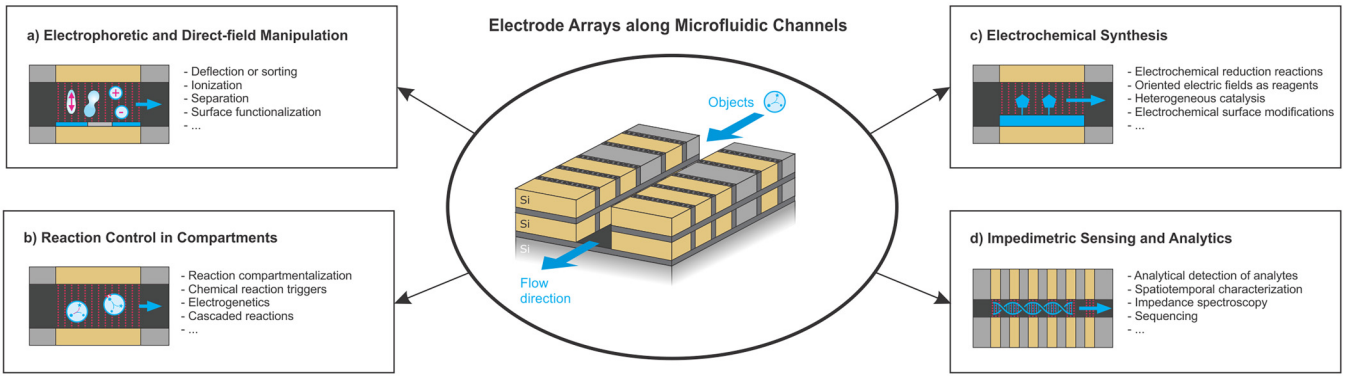


FIG. 3. Ultimately scaled, complex electrode arrays across and along microfluidic channels with some of the most prominent applications enabled by them: (a) Electrophoretic or direct, electric field-based manipulation. (b) Reaction control in micro- and nanoscale compartments. (c) Electrochemical synthesis. (d) Impedimetric sensing and analytics.

© Author(s) 2025

surface metallizations can be added toward the channel side and highly doped Si used as an electrode body. For many biochemical applications, however, such free charge carriers are usually undesired because they form radicals. For electrochemical applications, in contrast, electrons and holes are key to operation, acting both as reaction-initiating triggers and as probing species.

IV. ENVISIONED APPLICATIONS

The pivotal role of electric fields as triggers and modulators of chemical and biological processes is ubiquitous in nature, where local electric fields (LEFs) are key to controlling chemical reactions at the cellular, molecular, or even atomic level. For example, LEFs can guide the catalytic efficiency of enzymes whose catalytic processes are driven by electrostatic principles. Also, cellular processes are often regulated by constant or time-dependent LEFs induced through ion flow processes across cellular channel walls. With the scaling potentials discussed above, microfluidic devices will reach dimensions where the externally applied electric fields can be considered sufficiently "local" in the sense that spatially small cavities can be addressed. Another option is that channel dimensions are only one or two orders of magnitude larger than the dimensions of the objects present therein, which can be technically realized for droplets, cells, enzymes, or large molecules. This scenario may lead to a range of novel or drastically improved applications in the field of micro- and nanofluidics, for instance, the control of the regulatory capacity of cell-internal electric fields by cell-external electric fields.

Another example are electric field strengths that can reach amplitudes that can directly ionize objects, porate one object into another one, or interact with electrochemically modified surfaces. When LEFs are oriented and aligned with the chemical reaction axis, as is the case for heterogeneous catalysis with surface-bound, oriented molecular layers, they can become "smart reagents" in chemical synthesis. Here, LEFs not only trigger reactions by tunable and high electrochemical potentials, they allow also to govern control over stereoselectivity, chirality, etc. In turn, local micro- and nanoscale electrodes can be leveraged for sensing modalities to probe small objects or even object-internal dielectric or capacitive features. Here, we sketch out some of the most attractive near-term opportunities that are enabler by ultimately scaled, complex electrode arrays offered by the device fabrication approach presented and illustrated in Fig. 3.

A. Manipulation based on electrophoresis or direct particle–field interactions

Electrophoresis and dielectrophoresis are essential processes for manipulating and sorting micro-sized objects in microfluidic systems, as discussed above and demonstrated in the aforementioned proof-of-concept architecture.[14] The movement of mostly negatively charged objects toward a positively biased electrode can occur in either a direct current (DC) or alternating current (AC) field. DC deflection usually takes advantage of surface charges, while dielectrophoresis applies a non-uniform AC field to actuate particles based on their different polarizabilities. The resulting trajectories depend on the charge, polarizability, and the size of the objects. In down-scaled or high-field gradient geometries, droplets may be directly generated, more effectively polarized or even ionized. Also, a faster or larger deflection amplitude can be achieved in a microelectrode array. This translates into higher throughput rates and better control over the objects to be sorted. The handling of even smaller objects, such as single cells or molecules, will work, and injection or poration-like formation processes become realistic under high-field amplitudes and the long-term stable operation of silicon devices. In such cases, the delivery of DNA, RNA, and drug molecules into artificial or naturally occurring cells can be achieved by temporarily opening and closing the cell membrane through very short, high-intensity electrical pulses that create temporary pores in their membranes. Such electroporation can be leveraged to facilitate the delivery of genetic material into cells for gene editing or protein expression studies. Furthermore, encapsulation of cells into emulsion droplets can be utilized for various sorting applications[15–17] with higher speed and precision. The realization of quadrupolar field distributions within the channel cross section may lead to very effective filters for separation or filtering of smallest objects, also in gas-phase applications. For all these applications and miniaturizations, only silicon provides the required structural compliance and long-term stability. In addition to the electrical manipulation of objects in the channel, high fields and narrowly spaced electrodes may also be used to modify the microfluidic channel walls when coated with electrosensitive materials. This may lead, for instance, to tunable or switchable surface properties, such as wetting, referred to as electrowetting, at macroscopic dimensions.[18] Here, linearly arranged electrode arrays allow the precise manipulation of individual liquid droplets, which themselves function as solution-phase reaction chambers, as will be discussed below. Control over site-selective potentials allows microfluidic devices to be locally functionalized based on electrochemical multiplexing, a chemical engineering task that provides powerful means to expose different molecular functionalities to the channels. Examples of functional coatings include compound-selective receptors that enable sensing by capturing specific analytes. The electrical functionalization mechanisms combined with electrical addressing of individual channels provide effective means to functionalize entire chips by the flow-assembly. Figure 3(a) depicts, conceptually and highly simplified, some of the envisioned operations.

B. Reaction control in micro- and nanoscale compartments

Another nature-inspired concept used in microfluidics is the compartmentalization of reactions, realized in droplet microfluidics through oil–water droplets, double vesicles, or similar confinements. Flow-focusing devices enable the generation of such compartments in complex junctions where two or more phases merge and self-organize. The control over the compositions allows the assembly of compartments with well-defined content of multiple reagents. Enzymatic assays,[19] bioreaction pathway screening, parallel analysis, DNA sequencing,[20] and directed evolution are just a few of the many processes that have been demonstrated. This well-controlled environment provides optimized conditions for biochemical processes, such as, e.g., protein crystallization. Recently, double-membrane vesicles have reached an increased level of complexity, as they can be assembled from polymeric membranes,

© Author(s) 2025

making them more and more similar to a natural cell in terms of the designed functionalities. DNA-origami like ports have been embedded in the membrane,[21] and it is conceivable that electro-sensitive channels will soon be available in electrogenetics. For all these types of artificial reaction compartments, the interaction with external electric fields is highly interesting as it allows the triggering, modulation, and readout of reactions and processes occurring within the compartments or between several communicating compartments. Furthermore, droplets can be clustered, mass-flow exchange included, and the compartments can be separated again, all based solely on interactions with external or local electric fields.

C. Electrochemical synthesis

Similar to the operation within a compartment, chemical processes and operations can also be realized directly in electrified and functionalized micro- and nanochannels. Here, the field strengths and the orientation of the LEFs and their gradients are deterministically defined within the high-resolution electrode arrays. This scenario provides means for controlled electro-synthesis. In general, the high surface-to-volume ratio in microfluidic devices enhances the efficiency of chemical reactions, and the rapid heat and mass exchange allows for a stringent reaction control.[22] The electric fields and electrochemical potentials generated by the wall-embedded electrodes provide the best control over redox-reactions for chemical synthesis performed in a microflow reactor configuration. For such tasks, the aforementioned site-selective coating is again advantageous for creating the desired coating of reagents. Excellent means for screening surface coatings, e.g., for next-generation implants, regenerative medicine, and tissue engineering devices, as well as biosensors and drug delivery devices for disease diagnosis and treatment,[23] are provided by devices that offer multiple characterization sites. These can be probed under different conditions for an efficient screening on a scalable and reliable device platform. Novel possibilities are also expected for electrosynthesis working on the single or self-assembled mono-layer levels. Here, the availability of both high field strengths and oriented LEFs as being present, e.g., in the case of two opposite electrodes [Fig. 3(c)] where at least one is coated with the molecular layers, opens interesting avenues for synthesis. This allows directed electric fields to be used as smart reagents[24] in a flow reactor and not a scanning tunneling microscopy (STM) or atomic force microscopy (AFM) based configuration that is not scalable and difficult to be implemented in devices. For electrosynthesis, the local supply of electrons or holes is an interesting alternative to study chemical processes very locally, perhaps even monitored by appropriate techniques. Narrow electrode spacing may cause large concentration gradients that are otherwise not achievable with macroscopic or non-homogeneous fields.

D. Impedimetric sensing and analytics

The close placement of electrodes right at the solid–liquid (or solid–gas) interface, in the immediate vicinity of the objects present inside the micro- or nanofluidic channels, and the narrow spatial distances between the electrodes render such device geometries highly suitable for sensing applications. Since the channels can be scaled down in diameter to nearly the same dimensions as the objects passing through them, the electrical, electrochemical, capacitive, or impedimetric signals are maximized relative to the background of the medium. Due to the low impedance of the electrodes, such probes will be highly sensitive. What has not yet been exploited in microfluidics, due to the limited spatial resolution of current electrode implementations below 1 μm, is the high spatial resolution to probe different channel segments through an ultranarrow electrode array. Combined with the flow within the channels, unprecedented spatiotemporal resolution for sensing can be achieved, providing novel means for electrical tracking or feedback control of secondary tasks, e.g., deflection for sorting, rather than optical ones, which would be an increase in both throughput and efficiency. Such concepts would also not require labels, e.g., to provide fluorescence signals, making the approach more broadly applicable. Multiple electrodes arranged in close proximity give rise to multiplexing and hyperspectral sensing where AC-LEFs enable impedance changes caused by passing cells or biomolecules to be measured. This allows their properties, e.g., size or speed of the cell, DNA sequences, etc., to be inferred. Such biosensors[25] have already shown fast response times for larger electrode dimensions, minimal reagent consumption, and ease of handling without the need for any cellular pre-treatment or labeling, allowing even for mobile applications.[26,27] It is noteworthy that the electrode arrays are typically arranged in-plane, while optical transmission can additionally be realized orthogonally out-of-plane through viewports as mentioned in Sec. II. This gives rise to combined electro-optical sensing with various applications, e.g., an electrochemical DNA sensor combining polymerase chain reaction (PCR) amplification and electrochemical detection.[28]

E. Co-integration of microfluidics and CMOS technology on a silicon platform

The use of silicon as main microfluidic channel material opens interesting opportunities and synergies for a co-integration with CMOS technology; almost all electronic devices used today are based on CMOS technology and provide a large range of components and functionalities also suited for operating microfluidic devices as described above. Such components include, for example, passive and active voltage and current sources that can all be controlled by microprocessors. They can supply voltage or current to the electrodes (with the typical amplitudes of 0–10 V now an acceptable dynamic range for CMOS circuits thanks to the nearby electrodes) and respond with very little delay due to the short communication distances and the use of real-time logics running on the microprocessors on the same board. Furthermore, sensing components can be deployed from the silicon stack as well, including photodetectors, photomultipliers, or amplifiers. They may provide input signals for real-time signal processing, e.g., to drive the deflection of the electrodes based on an optical input signal for ultrahigh throughput operation beyond 2 kHz. Meanwhile, even light sources can directly and monolithically be integrated on a silicon platform, such that they can act, e.g., as excitation triggers for FACS or FADS. Therefore, the entire FACS or FADS instrument can be realized in a small-form-factor device. Also micro-electromechanical devices, typically made out of SOI wafers, can act as valves to route liquids or simply mix media in addition to

© Author(s) 2025

other applications. Last, also, communication modules are available on the CMOS platform, using energy-efficient protocols and communication standards, such as low-energy Bluetooth. This will eventually enable such novel devices to be integrated as smart, Internet-of-things instruments.

All the processes required for the microfluidic part are scalable, and no exotic processes are used. As this fabrication does not need last-node requirements, the devices can be relatively cheaply fabricated in a standard clean room. Still, the fabrication can be scaled up to large wafer scales, which will reduce the cost of mass-production. As the silicon chips have virtually no fatigue and can be cleaned even under harsh conditions, they have a substantially longer lifetime than other approaches.

The integration of silicon microfluidics with electronics and optics fabricated also on a silicon platform can be realized in various ways. The DRIE of the deep microfluidic channels as well as the anodic bonding are not directly backend-of-line-compatible processes in CMOS. Therefore, the simplest solution would be to stack the chips on top of each other (e.g., by using conventional solder joints to establish electrical and mechanical connection) or to assemble individual chiplets side by side, which would be easier if waveguides are involved for light transmission. Irrespective of these technical solutions already available from other concepts, the overall system will lead to drastic miniaturization of devices, which can be deployed both in laboratory environments and mobile applications.

V. CONCLUSIONS

The direct electrification of channel walls in silicon microfluidic devices provides stable and reliable means of electrically addressing a microfluidic channel segment. The optimal electrostatic geometries allow low-voltage or high-field operation with either highly homogeneous electric fields or high field gradients. The fabrication approach allows dimensional and complexity scaling. This provides the means for more efficient manipulation, more stringent reaction control in compartments, field-based electrochemistry or electrical sensing, all with increased speed and control of smaller and smaller objects down to single cells, proteins, or molecules. In particular, all of the above-mentioned building blocks can be arranged in a highly complex 3D fluid network by stacking silicon or glass layers on top of each other to create multifunctional devices with various functionalities on the very same chip. From a fabrication perspective, the compatibility with CMOS allows monolithic integration and direct use of CMOS functionalities. This in turn could provide new applications in point-of-care healthcare, medicine, personalized medicine, and more.

ACKNOWLEDGMENTS

The authors gratefully acknowledge financial support from the National Centre of Competence in Research Molecular Systems Engineering (NCCR-MSE, Grant No. 51NF–40–205608). This work was supported by the Swiss State Secretariat for Education, Research and Innovation (SERI) under Contract No. 22.00034 (Horizon Europe Research and Innovation Project CORENET). The authors further appreciated scientific discussion with M. Mayor, S. Panke, C. Palivan, M. Fussenegger, C. Spar, D. Ward, D. Widmer, and H. Wolf as well as strategic support from B. Gotsmann, H. Riel, and A. Curioni.

This work was funded by the European Union and supported by the Swiss State Secretariat for Education, Research and Innovation (SERI) under Contract Nos. 22.00017 and 22.00034. Views and opinions expressed are, however, those of the author(s) only and do not necessarily reflect those of the European Union or the European Innovation Council and SMEs Executive Agency (EISMEA). Neither the European Union nor the granting authority can be held responsible for them.

AUTHOR DECLARATIONS

Conflict of Interest

E.L. has U.S. Patent Application 2022/135399 A1 (Ref. 13), published and granted on 2023-06-13 as US11673798B2. The remaining authors have no conflicts to disclose.

Author Contributions

K.-S. Csizi: Conceptualization (equal); Methodology (equal); Writing – original draft (equal); Writing – review & editing (equal). **A. E. Frackowiak:** Conceptualization (equal); Investigation (equal); Writing – original draft (equal). **R. D. Lovchik:** Investigation (equal). **E. Lörtscher:** Conceptualization (equal); Funding acquisition (equal); Investigation (equal); Methodology (equal); Project administration (equal); Resources (equal); Supervision (equal); Validation (equal); Visualization (equal); Writing – original draft (equal); Writing – review & editing (equal).

DATA AVAILABILITY

Data sharing is not applicable to this article as no new data were created or analyzed in this study.

REFERENCES

[1]X. Ding, P. Li, S.-C. S. Lin, Z. S. Stratton, N. Nama, F. Guo, D. Slotcavage, X. Mao, J. Shi, F. Costanzo, and T. J. Huang, "Surface acoustic wave microfluidics," Lab Chip **13**, 3626–3649 (2013).

[2]S. Zhang, B. Xu, M. Elsayed, F. Nan, W. Liang, J. K. Valley, L. Liu, Q. Huang, M. C. Wu, and A. R. Wheeler, "Optoelectronic tweezers: A versatile toolbox for nano-/micro-manipulation," Chem. Soc. Rev. **51**, 9203–9242 (2022).

[3]K. Ahn, C. Kerbage, T. P. Hunt, R. M. Westervelt, D. R. Link, and D. A. Weitz, "Dielectrophoretic manipulation of drops for high-speed microfluidic sorting devices," Appl. Phys. Lett. **88**, 024104 (2006).

[4]E. Brouzes, M. Medkova, N. Savenelli, D. Marran, M. Twardowski, J. B. Hutchison, J. M. Rothberg, D. R. Link, N. Perrimon, and M. L. Samuels, "Droplet microfluidic technology for single-cell high-throughput screening," Proc. Natl. Acad. Sci. U.S.A. **106**, 14195–14200 (2009).

[5]L. Mazutis, J.-C. Baret, P. Treacy, Y. Skhiri, A. F. Araghi, M. Ryckelynck, V. Taly, and A. D. Griffiths, "Multi-step microfluidic droplet processing: Kinetic analysis of an *in vitro* translated enzyme," Lab Chip **9**, 2902–2908 (2009).

[6]L. Rao, B. Cai, X.-L. Yu, S.-S. Guo, W. Liu, and X.-Z. Zhao, "One-step fabrication of 3D silver paste electrodes into microfluidic devices for enhanced droplet-based cell sorting," AIP Adv. **5**, 057134 (2015).

[7]A. Sciambi and A. R. Abate, "Generating electric fields in PDMS microfluidic devices with salt water electrodes," Lab Chip **14**, 2605–2609 (2014).

© Author(s) 2025

[8]J. Park, B. Kim, S. K. Choi, S. Hong, S. H. Lee, and K.-I. Lee, "An efficient cell separation system using 3D-asymmetric microelectrodes," Lab Chip **5**, 1264–1270 (2005).
[9]N. Lewpiriyawong and C. Yang, "AC-dielectrophoretic characterization and separation of submicron and micron particles using sidewall AgPDMS electrodes," Biomicrofluidics **6**, 012807 (2012).
[10]X. Niu, M. Zhang, S. Peng, W. Wen, and P. Sheng, "Real-time detection, control, and sorting of microfluidic droplets," Biomicrofluidics **1**, 044101 (2007).
[11]N. Lewpiriyawong, C. Yang, and Y. C. Lam, "Continuous sorting and separation of microparticles by size using AC dielectrophoresis in a PDMS microfluidic device with 3-D conducting PDMS composite electrodes," Electrophoresis **31**, 2622–2631 (2010).
[12]M. A. Saucedo-Espinosa and P. S. Dittrich, "In-droplet electrophoretic separation and enrichment of biomolecules," Anal. Chem. **92**, 8414–8421 (2020).
[13]G. F. Puebla Hellmann, D. Monserrat Lopez, U. Drechsler, M. Mayor, and E. Lörtscher, "Microfluidic devices with electrodes formed as physically separated sections of microchannel side walls," US patent application 2022/135399 A1 (2022).
[14]D. Monserrat Lopez, P. Rottmann, G. Puebla-Hellmann, U. Drechsler, M. Mayor, S. Panke, M. Fussenegger, and E. Lörtscher, "Direct electrification of silicon microfluidics for electric field applications," Microsyst. Nanoeng. **9**, 81 (2023).
[15]F. Guo, X.-H. Ji, K. Liu, R.-X. He, L.-B. Zhao, Z.-X. Guo, W. Liu, S.-S. Guo, and X.-Z. Zhao, "Droplet electric separator microfluidic device for cell sorting," Appl. Phys. Lett. **96**, 193701 (2010).
[16]L. Mazutis, J. Gilbert, W. L. Ung, D. A. Weitz, A. D. Griffiths, and J. A. Heyman, "Single-cell analysis and sorting using droplet-based microfluidics," Nat. Protoc. **8**, 870–891 (2013).
[17]R. S. W. Thomas, P. D. Mitchell, R. O. C. Oreffo, H. Morgan, and N. G. Green, "Image-based sorting and negative dielectrophoresis for high purity cell and particle separation," Electrophoresis **40**, 2718–2727 (2019).
[18]Y. Arango, Y. Temiz, O. Gökce, and E. Delamarche, "Electrogates for stop-and-go control of liquid flow in microfluidics," Appl. Phys. Lett. **112**, 153701 (2018).
[19]E. M. Miller and A. R. Wheeler, "A digital microfluidic approach to homogeneous enzyme assays," Anal. Chem. **80**, 1614–1619 (2008).
[20]B. M. Paegel, R. G. Blazej, and R. A. Mathies, "Microfluidic devices for DNA sequencing: Sample preparation and electrophoretic analysis," Curr. Opin. Biotechnol. **14**, 42–50 (2003).
[21]R. Cochereau, V. Maffeis, E. C. dos Santos, E. Lörtscher, and C. G. Palivan, "Polymeric giant unilamellar vesicles with integrated DNA-origami nanopores: An efficient platform for tuning bioreaction dynamics through controlled molecular diffusion," Adv. Funct. Mater. **33**, 2304782 (2023).
[22]T. Noël, Y. Cao, and G. Laudadio, "The fundamentals behind the use of flow reactors in electrochemistry," Acc. Chem. Res. **52**, 2858–2869 (2019).
[23]A. P. Quist and S. Oscarsson, "Micropatterned surfaces: Techniques and applications in cell biology," Expert Opin. Drug Discov. **5**, 569–581 (2010).
[24]S. Shaik, D. Mandal, and R. Ramanan, "Oriented electric fields as future smart reagents in chemistry," Nat. Chem. **8**, 1091–1098 (2016).
[25]Y.-S. Chen, C.-H. Huang, P.-C. Pai, J. Seo, and K. F. Lei, "A review on microfluidics-based impedance biosensors," Biosensors **13**, 83 (2023).
[26]L. Yang, Z. Zhang, and X. Wang, "A microfluidic pet-based electrochemical glucose sensor," Micromachines **13**, 552 (2022).
[27]M. Zhang, X. Yang, M. Ren, S. Mao, R. Dhakal, N.-Y. Kim, Y. Li, and Z. Yao, "Microfluidic microwave biosensor based on biomimetic materials for the quantitative detection of glucose," Sci. Rep. **12**, 15961 (2022).
[28]B. S. Ferguson, S. F. Buchsbaum, J. S. Swensen, K. Hsieh, X. Lou, and H. T. Soh, "Integrated microfluidic electrochemical DNA sensor," Anal. Chem. **81**, 6503–6508 (2009).

© Author(s) 2025